THE PROTEIN SOCIETY

Crystal structure and calcium-induced conformational changes of diacylglycerol kinase α EF-hand domains

Daisuke Takahashi,[1] Kano Suzuki,[1] Taiichi Sakamoto,[2] Takeo Iwamoto,[3] Takeshi Murata,[1,4] and Fumio Sakane[1]*

[1]Department of Chemistry, Graduate School of Science, Chiba University, Chiba, Japan
[2]Department of Life Science, Faculty of Advanced Engineering, Chiba Institute of Technology, Chiba, Japan
[3]Division of Molecular Cell Biology, Core Research Facilities for Basic Science, Research Center for Medical Sciences, The Jikei University School of Medicine, Chiba, Japan
[4]Molecular Chirality Research Center, Chiba University, Chiba, Japan

Received 4 December 2018; Accepted 10 January 2019
DOI: 10.1002/pro.3572
Published online 17 January 2019 proteinscience.org

Abstract: **Diacylglycerol kinases (DGKs) are multi-domain lipid kinases that phosphorylate diacylglycerol into phosphatidic acid, modulating the levels of these key signaling lipids. Recently, increasing attention has been paid to DGKα isozyme as a potential target for cancer immunotherapy. We have previously shown that DGKα is positively regulated by Ca^{2+} binding to its N-terminal EF-hand domains (DGKα-EF). However, little progress has been made for the structural biology of mammalian DGKs and the molecular mechanism underlying the Ca^{2+}-triggered activation remains unclear. Here we report the first crystal structure of Ca^{2+}-bound DGKα-EF and analyze the structural changes upon binding to Ca^{2+}. DGKα-EF adopts a canonical EF-hand fold, but unexpectedly, has an additional α-helix (often called a ligand mimic [LM] helix), which is packed into the hydrophobic core. Biophysical and biochemical analyses reveal that DGKα-EF adopts a protease-susceptible "open" conformation without Ca^{2+} that tends to form a dimer. Cooperative binding of two Ca^{2+} ions dissociates the dimer into a well-folded monomer, which resists to proteolysis. Taken together, our results provide experimental evidence that Ca^{2+} binding induces substantial conformational changes in DGKα-EF, which likely regulates intra-molecular interactions responsible for the activation of DGKα and suggest a possible role of the LM helix for the Ca^{2+}-induced conformational changes.**

Abbreviations: ATP, adenosine triphosphate; CD, catalytic domain; DG, diacylglycerol; DGK, diacylglycerol kinase; ITC, isothermal titration calorimetry; LM helix, ligand mimic helix; PA, phosphatidic acid; RVH, recoverin homology; SAD, single-wavelength anomalous dispersion; SEC, size-exclusion chromatography; TNS, 2-p-toluidinylnaphthalene-6-sulphonate.

Additional Supporting Information may be found in the online version of this article.

Grant sponsor: Chiba University Association of Graduate Schools of Science and Tec; Grant sponsor: Japan Agency for Medical Research and Development Platform Project for Supporting Drug Discovery and JP18am0101083; Grant sponsor: Japan Society for the Promotion of Science Grant-in-Aid for Scientific Research/17K115444 to Grant-in-Aid for Scientific Research/18H05425 to T Grant-in-Aid for Scientific Research/26291017, 15K 17H03650 15K14470 26291017 18H05425 17K115444; Grant sponsor: The Asahi Group Foundation; Grant sponsor: The Food Science Institute Foundation; Grant sponsor: The Futaba Electronic Memorial Foundation; Grant sponsor: The Japan Foundation for Applied Enzymology; Grant sponsor: The Japan Milk Academic Alliance; Grant sponsor: the Ono Medical Research Foundation; Grant sponsor: The Skylark Food Science Institute; Grant sponsor: Japan Milk Academic Alliance; Grant sponsor: Asahi Group Foundation; Grant sponsor: Skylark Food Science Institute; Grant sponsor: Japan Foundation for Applied Enzymology; Grant sponsor: Ono Medical Research Foundation; Grant sponsor: Futaba Electronic Memorial Foundation.

**Correspondence to*: Fumio Sakane, Department of Chemistry, Graduate School of Science, Chiba University, 1-33 Yayoi-cho, Inage-ku, Chiba 263-8522, Japan. E-mail: sakane@faculty.chiba-u.jp

Daisuke Takahashi's current address is Department of Pharmaceutical Health Care and Sciences, Kyushu University, Fukuoka, Japan.

Significance statement: **Diacylglycerol kinases (DGKs), which modulates the levels of two lipid second messengers, diacylglycerol and phosphatidic acid, is still structurally enigmatic enzymes since its first identification in 1959. We here present the first crystal structure of EF-hand domains of diacylglycerol kinase α in its Ca^{2+} bound form and characterize Ca^{2+}-induced conformational changes, which likely regulates intra-molecular interactions. Our study paves the way for future studies to understand the structural basis of DGK isozymes.**

Keywords: diacylglycerol kinases; DGKα; EF-hand domains; calcium binding; a ligand mimic helix; crystal structure; conformational changes

Introduction

While existing as a minor lipid component in cell membranes, signaling lipids play a key role in a plethora of cellular events, and their levels are dynamically and tightly controlled by lipid-metabolizing enzymes such as phospholipases, lipid phosphatases, and lipid kinases. Diacylglycerol kinase (DGK) is one such lipid kinase that catalyzes the adenosine triphosphate (ATP)-dependent phosphorylation of diacylglycerol (DG) to phosphatidic acid (PA).[1–3] Both DG and PA serve as second messengers, and activate and modulate a number of signaling proteins[4–7] including (i) protein kinase C (PKC) isoforms[5,8,9] and Ras guanyl nucleotide-releasing protein (RasGRP)[10,11] by DG, and (ii) mammalian target of Rapamycin (mTOR)[12] and phosphatidylinositol (PI)-4-phosphate 5-kinase (PIP5K)[13] by PA. Hence, DGK functions as a molecular hub for many signaling events by terminating/attenuating DG signaling and activating PA signaling.[1,2]

Among 10 mammalian isozymes of DGK (α, β, γ, δ, η, κ, ε, ζ, ι, and θ) identified so far,[1,3] DGKα has recently been recognized as a potential target for anti-cancer treatments including cancer immunotherapy.[14–18] The expression of DGKα has been found upregulated in various types of cancer cells including melanoma cells (but not in non-cancerous melanocytes),[19] lymphoma,[20] hepatocellular carcinoma,[21] breast cancer cells,[22] and glioblastoma cells[18] where DGKα promotes cancer cell survival, proliferation, migration, and invasion.[23] In T-lymphocytes, on the other hand, DGKα is known as a critical attenuator for cellular immunity. DGKα is highly expressed in T-cells and terminates DG signaling critical for RasGRP1-dependent activation of the Ras–Erk pathway.[24] Furthermore, *in vitro* and *in vivo* studies have uncovered that DGKα is responsible for T-cell hyporesponsive state known as the anergy state.[25,26] Therefore, as exemplified in our and other studies, a DGKα inhibitor not only has detrimental effects on cancer cells by inducing apoptosis,[16,18] but stimulates the production of Interleukin-2 in Jurkat T cells,[16] which may potentially restore the anti-tumor function of T-cells. This evidence strongly suggests that a DGKα-selective inhibitor can possibly be utilized for cancer immunotherapy.[14] However, little progress has been made in understanding the structural biology of mammalian DGKs. No structures of DGKα catalytic and regulatory domains have been reported, impeding the development and optimization of effective DGKα inhibitors.

DGKα is a Type I DGK isozyme and contains multiple domains including a recoverin homology (RVH) domain, a pair of EF-hand domains (EF), two cysteine-rich, zinc finger-like regions called C1 domains (C1), and a carboxyl-terminal catalytic domain (CD) [Fig. 1(a)].[27] This modular structure is believed to be responsible for enzymatic properties and cellular localizations.[1,2] Among those modules, the EF-hand domain can bind calcium and has been long known to activate and modulate Ca^{2+} signaling events or control Ca^{2+} homeostasis.[28–30] Accumulating evidence has demonstrated a pivotal role played by the EF-hands of DGKα (DGKα-EF) in regulating the enzymatic activity of DGKα. Our previous studies have shown that DGKα purified from porcine thymus binds calcium with a stoichiometry of 2 moles of Ca^{2+} per mole of the enzyme, and that the Ca^{2+} binding to DGKα-EF activates the enzyme.[31–33] We and others have also revealed that the truncation of RVH and EF-hand domains constitutively activates DGKα, irrespective of whether calcium is present or not.[32,34] Furthermore, Ca^{2+} binding is critical for DGKα to translocate to the membrane.[31] Merino et al. have shown that deletion of N-terminal domains leads to constitutive localization of the DGKα mutant to the plasma membrane in T-cells.[35]

To advance our understanding of the structural basis for the Ca^{2+}-dependent activation of DGKα, we here report the first crystal structure of human DGKα-EF in its Ca^{2+} bound form and characterize the Ca^{2+} binding to DGKα-EF and the conformational changes triggered by Ca^{2+} binding.

Results

Structure determination of DGKα-EF with Ca^{2+}

DGKα-EF [aa 107–197 of the mature protein; Figure 1(a)] with N-terminal His_6-SUMO tag was expressed in *Escherichia coli* cells and purified from soluble cell lysate using Ni-affinity chromatography. After cleavage of His_6-SUMO tag with ubiquitin-like specific protease (Ulp1), DGKα-EF in a tag-free form could be purified to homogeneity using Ni-affinity chromatography followed by size-exclusion chromatography (SEC) in the presence of 5 m*M* $CaCl_2$. The

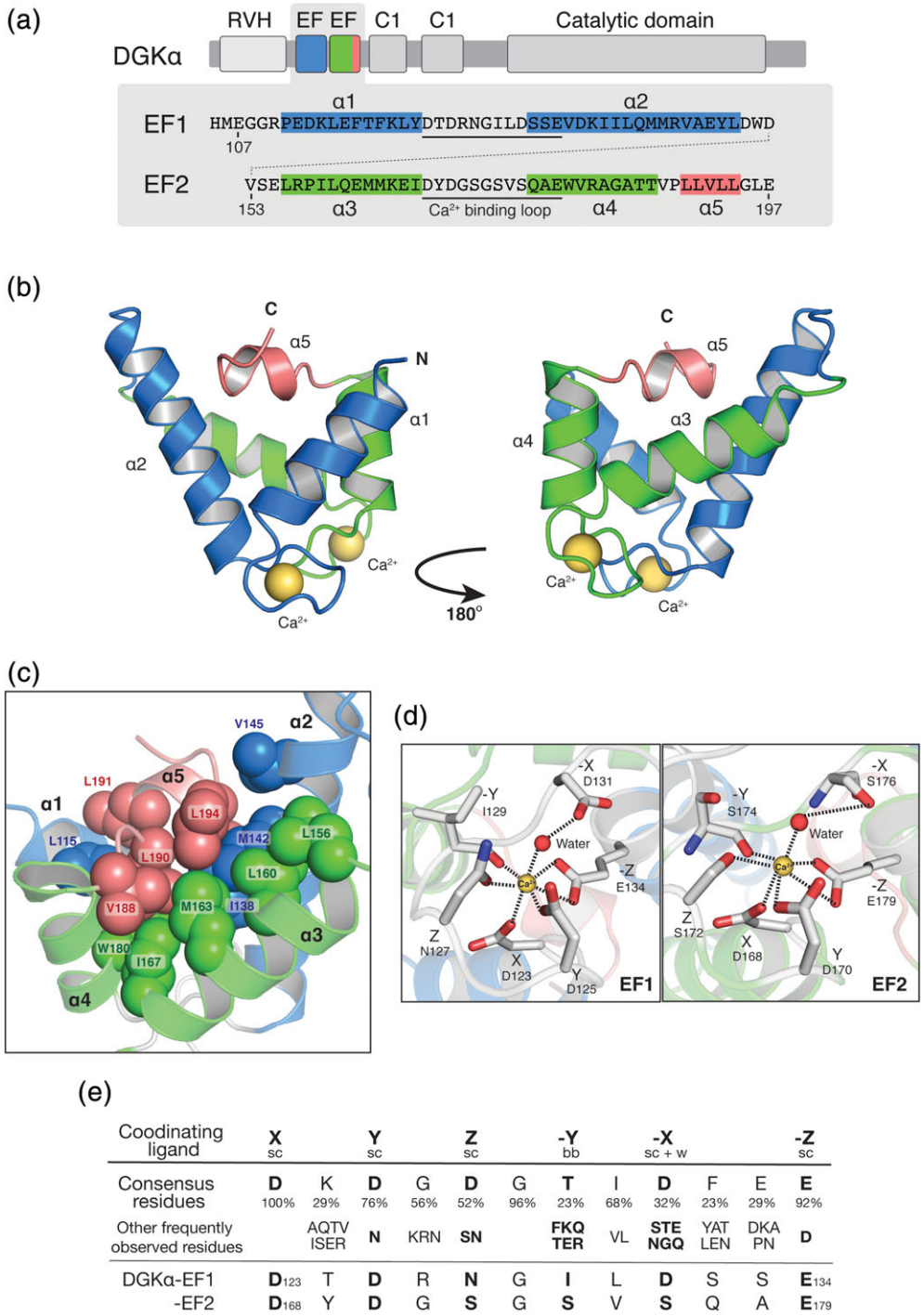

(e)

Coodinating ligand	X sc		Y sc		Z sc		-Y bb		-X sc + w			-Z sc
Consensus residues	**D** 100%	K 29%	**D** 76%	G 56%	**D** 52%	G 96%	**T** 23%	I 68%	**D** 32%	F 23%	E 29%	**E** 92%
Other frequently observed residues		AQTV ISER	**N**	KRN	**SN**		**FKQ TER**	VL	**STE NGQ**	YAT LEN	DKA PN	**D**
DGKα-EF1	**D_{123}**	T	**D**	R	**N**	G	**I**	L	**D**	S	S	**E_{134}**
-EF2	**D_{168}**	Y	**D**	G	**S**	G	**S**	V	**S**	Q	A	**E_{179}**

Figure 1. Crystal structure of the Ca^{2+}-bound DGKα-EF. (a) Domain architecture of human DGKα. DGKα consists of the N-terminal regulatory domains including recoverin homology domain (RVH), a pair of EF-hand motifs (DGKα-EF) and cysteine-rich, the protein kinase C conserved Region 1(C1) domains, and the C-terminal catalytic domain. RVH is related to the amino terminus of the recoverin family of neuronal calcium sensors.[34] Shown below is the sequence of DGKα-EF (aa 107–197). Helices (α1–α4) are marked by blue (α1– α2), green (α3– α4), and pink (α5). Residues involved in Ca^{2+} coordination (Ca^{2+}-binding loop) are underlined. (b) Ribbon representation of the overall structure of the Ca^{2+}-bound DGKα-EF. EF1 and EF2 are shown in blue and green colors, respectively. The α5 helix is in pink. Yellow sphere indicates calcium. (c) Hydrophobic interactions involving the α5 LM helix with other helices in DGKα-EF. Hydrophobic residues are shown as sphere and labeled. (d) Close-up view of the Ca^{2+}-binding sites in EF1 (left) and EF2 (right). Ca^{2+} coordinating residues are shown as sticks and labeled. Ca^{2+} coordination bonds are highlighted with dashed lines. (e) Consensus and DGKα sequences of EF-hand Ca^{2+} binding loops. Ca^{2+} ligands are indicated with the coordination positions (*X*, *Y*, *Z*, *–X*, *–Y*, and *–Z*).[36] Ca^{2+} is coordinated via side chain (sc) or through the backbone (bb) of the amino acids. The amino acid residue at *–X* is typically hydrogen-bonded to a water molecule that coordinates Ca^{2+} and indicated with "sc + w". The percentage of occurrence for consensus residues (%) and other frequently observed residues are also shown.

Table I. *Data Collection and Refinement Statistics*

		Native	S-SAD
Data collection			
	Beamline	PF BL-1A	PF BL-1A
	Wavelength (Å)	1.1	2.7
	Exposure time (s)	0.2	0.05
	Oscillation angle (°)	0.5	0.1
	Total oscillation range (°)	350	1440
	Space group	$P3_221$	$P3_221$
	Cell dimensions		
	a, *b*, *c* (Å)	58.19, 58.19, 61.12	57.22, 57.22, 60.33
	α, β, γ (°)	90, 90, 120	90, 90, 120
	Resolution (Å)	50–2.14 (2.27–2.14)	50–2.75 (2.82–2.75)
	No. reflections	66,449 (10,661)	195,653 (1571)
	Rmerge	0.083 (0.661)	0.143 (6.261)
	$I/\sigma I$	15.13 (2.91)	15.54 (0.10)
	Completeness (%)	99.9 (99.2)	98.5 (80.3)
	Redundancy	9.7 (9.9)	34.4 (4.6)
Refinement			
	Resolution (Å)	50–2.14	
	Rwork/Rfree (%)	0.185 / 0.238	
	R.m.s deviations		
	Bond lengths (Å)	0.013	
	Bond angles (°)	1.315	

protein eluted from a SEC column in a volume of 83 mL corresponding to the DGKα-EF monomer (11 kDa) and was used for crystallization. The crystals of DGKα-EF with $CaCl_2$ belong to space group $P3_221$. The crystal structure of DGKα-EF was solved by the single-wavelength anomalous dispersion (SAD) utilizing five intrinsic sulfur atoms in the native protein and was refined at a 2.1 Å with final R_{work} and R_{free} factors of 18.5% and 23.8%, respectively. Data collection and refinement statistics are reported in Table I. Electron density map (2Fo-Fc maps) of a representative view of DGKα-EF is shown in Figure S1.

Crystal structure of the Ca^{2+}-bound DGKα-EF

The structure reveals that DGKα-EF is a canonical dimeric pair of helix-loop-helix EF-hand motifs and binds two Ca^{2+} ions [Fig. 1(b)]. Notably, the exiting helices (α4 and α5) of the second EF-hand motif (EF2) are interrupted by P189, and consequently, the short α5 helix lies almost perpendicular to α4 [Fig. 1(b)]. The α5 helix consisting of L190–L191–V192–L193–L194 is hydrophobic in nature and tightly packed into a hydrophobic core composed of L115 from α1, I138, M142 from α2, L160, M163, I167 from α3, and W180 in α3 [Fig. 1(c)]. In terms of Ca^{2+} binding, each Ca^{2+} ion in EF1 and EF2 is coordinated by several acidic residues along with other residues and water molecule (D123, D125, N127, I129, D131, E134 for EF1, D168, D170, S172, S174, and E179 for EF2) [Fig. 1(d)], which are aligned well with Ca^{2+}-coordinating residues conserved in other EF-hand domains (denoted as *X*, *Y*, *Z*, *–Y*, *–X*, and *–Z*) [Fig. 1(e)],[36] indicating that DGKα-EF binds to Ca^{2+} via canonical coordinating mechanism. The inter-helical angles between the entering and exiting helices are 68.75° for EF1 (between α1 and α2) and 64.4° for EF2 (between α3 and α4), respectively, well within the range for other EF-hand proteins.[28,37]

Since DGKα-EF is the first 3D structure determined for DGK Type I isozymes, structural alignment was conducted using the Dali server[38] to search structurally similar proteins in the PDB. The search produced several hits with high Z scores (defined as a strong match) as shown in Table S1. The most structurally similar structures include a Ca^{2+}-dependent protein kinase (*Z* score = 9, PDB ID 3mse), calaxin (*Z* = 8.7, 5×9a),[39] calmodulin-like domain protein kinase (*Z* = 8.6, 4ysm), L-plastin (*Z* = 8.4, 5joj),[40] and EFhd/Swiprosin (*Z* = 8.1, 5j2l)[41]. Strikingly, an extra helix as observed in EF2 of DGKα-EF (α5) also presents in a certain number of those structural homologs such as calaxin,[39] L-plastin,[40] EFhd/Swiprosin,[41] and mitochondrial Rho (Miro) EF-hand and GTPase domains from human[42] and *Drosophila*.[43] The extra helix has been previously proposed as a ligand mimic (LM) helix, since it is structurally reminiscent of several EF-hand motifs bounds to their ligands.[43] Representative EF-hand structures with the LM helix are shown in Figure S2.

We next analyzed the surface area of DGKα-EF in its Ca^{2+}-bound form for hydrophobicity. Notably, large hydrophobic patches are clustered and exposed to the top side of the protein, as shown in Figure 2, to which neighboring RVH and C1 domains are likely adjacent. This suggests the possible involvement of clustered hydrophobic inter-domain interactions in the context of the full-length protein. Of note, P189 and L193 in the LM helix, not packed in the hydrophobic core, are also exposed to form the hydrophobic surface.

Calcium ions cooperatively bind to DGKα-EF

We next used isothermal titration calorimetry (ITC) to characterize the calcium binding mode and thermodynamics of DGKα-EF. Ca^{2+} binding to wild-type DGKα-EF was found to be an exothermic process [Fig. 3(a)] with the binding stoichiometry of $n = 2$, which is consistent with the crystal structure of Ca^{2+}-bound DGKα-EF (Fig. 1). The binding isotherm can best fit with a sequential binding model with slightly different dissociation constants ($K_d^1 = 0.3$ μM and $K_d^2 = 2.3$ μM) [Fig. 3(a)]. Respective thermodynamic parameters are also shown in Table II. The obtained K_d values are comparable with the value previously measured with a full-length DGKα purified from pig thymus ($K_d = 0.3$ μM)[31] and slightly lower than those reported in another study in which a refolded and partially purified DGKα-EF was used ($K_d = 9.9$ μM).[33] Next, we evaluated two site-directed DGKα-EF mutants (E134Q and E179Q) where a calcium coordinating glutamic acid at the *–Z* position in EF1 and EF2 [Fig. 1(e)] was replaced with a glutamine by site-directed mutagenesis. For mutants, titration of $CaCl_2$ into E134Q mutant displayed an exothermic binding process with much less heat changes compared with WT [Fig. 3(b)]. The binding stoichiometry was 0.96 and the binding affinity ($K_d = 31.7$ μM) is significantly weaker than that of WT, indicating that a single Ca^{2+} ion can bind to DGKα-EF, most likely to EF2. In contrast, no heat changes were observed for E179Q [Fig. 3(c)], indicating that the mutation of E179 in the Ca^{2+}-binding loop of EF2 abolishes Ca^{2+} binding. Collectively, these results reveal that DGKα-EF binds to two Ca^{2+} ions in a cooperative manner and the two binding sites in EF1 and EF2 are asymmetric with EF2 most likely being the first Ca^{2+} binding site. As illustrated for other EF-hand Ca^{2+} sensor proteins,[36] this cooperative binding mode would allow DGKα-EF to quickly respond to changes in intracellular Ca^{2+} concentration, which increases from 100 nM to 10 μM upon stimulation.

Calcium binding induces a conformational change of DGKα-EF

We next probed the effect of Ca^{2+} binding on conformational and/or oligomerization state of DGKα-EF using SEC. Purified DGKα-EF was extensively dialyzed a buffer containing 3 m*M* EGTA to chelate-bound calcium ions, and applied to SEC. Interestingly, DGKα-EF in its apo-form eluted in a volume corresponding to 23.5 kDa, approximately twice the theoretical mass of DGKα-EF monomer (10.6 kDa) [Fig. 4(a,b)]. Dependence of the elution on protein concentration was also tested, and we found that DGKα-EF still eluted in a dimer volume when a diluted protein sample [0.07 mg/mL (6.6 μM)] was applied [Fig. 4(c)]. With lower concentrations of $CaCl_2$

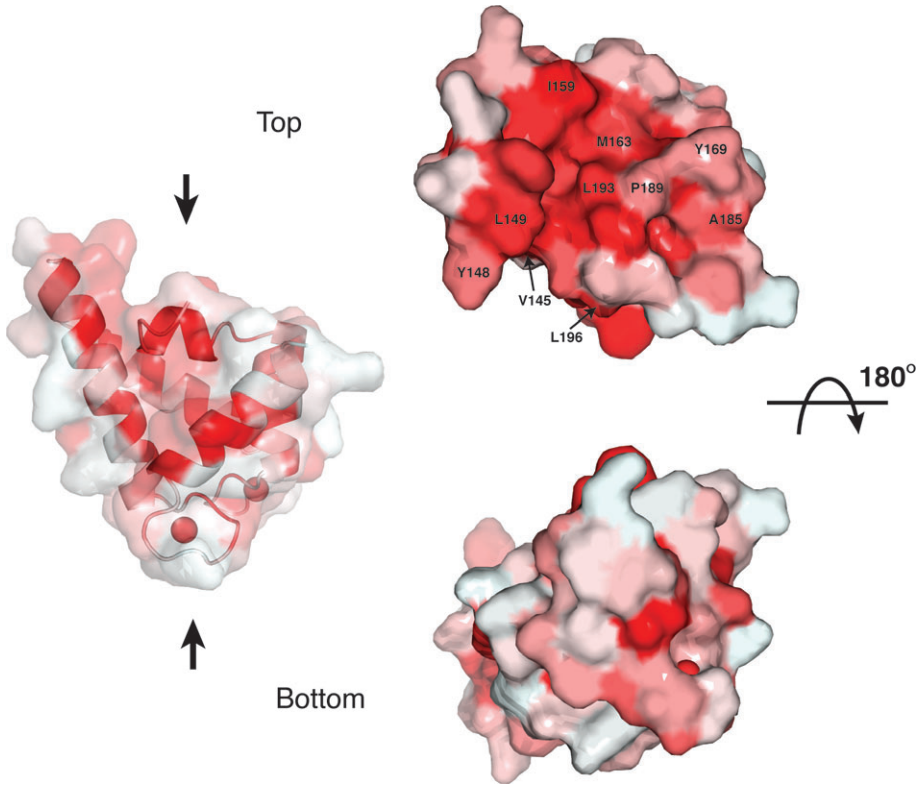

Figure 2. Structural characterization of the Ca^{2+}-bound DGKα-EF. Surface hydrophobicity was mapped using the color_h.py python script in PyMOL. Hydrophilic residues are in lighter and white color, and hydrophobic residues are labeled and shown in darker and red color.

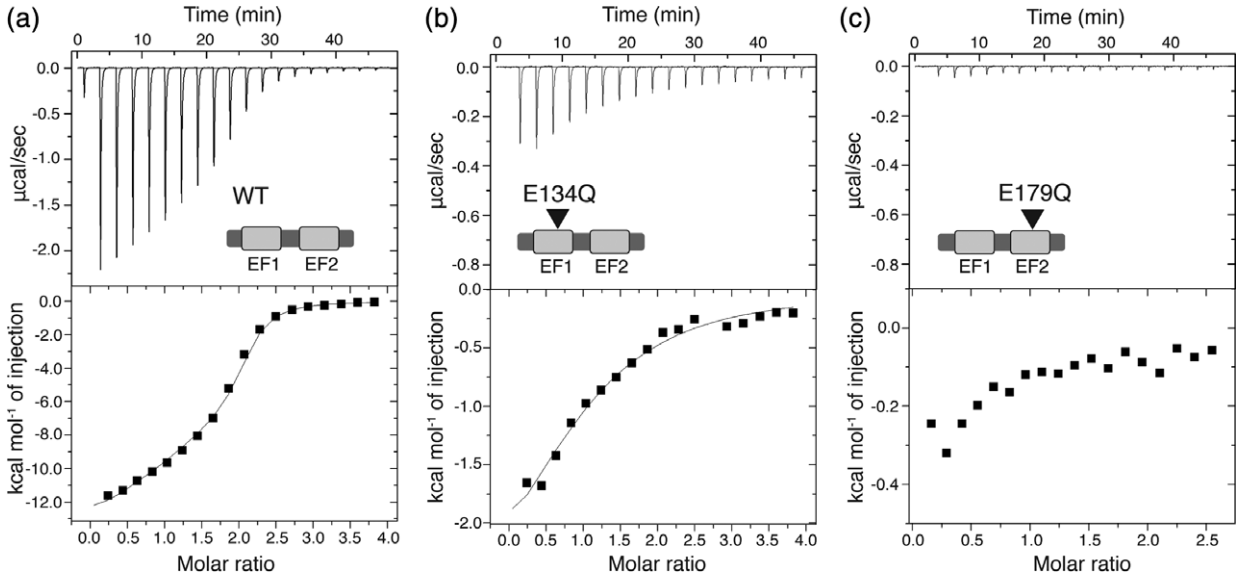

Figure 3. Isothermal titration calorimetry (ITC) analysis of calcium binding to DGKα-EF WT (a) and its mutants, E134Q (b) and E179Q (c). The upper panels show a representative thermogram. The lower panels show the integrated heat changes and the solid lines represent the fit of the data to a sequential binding model for WT and an N-identical binding site model for E134Q. Thermodynamic parameters are shown in Table II.

(0.2 and 0.5 μM), the elution volume of DGKα-EF slightly shifted to longer retention times corresponding to 21.7 kDa and 19.6 kDa [Fig. 4(a)], which are still within the range of DGKα-EF dimer. SEC analysis with higher $CaCl_2$ concentrations (2–50 μM) demonstrated that DGKα-EF predominantly eluted in a volume corresponding to its monomer (11 kDa) with small population being eluted in its dimer position. With 200 μM $CaCl_2$, the protein predominantly eluted as a monomer. These results suggest that the apo-DGKα-EF forms a dimer and Ca^{2+} binding induces a conformational change to dissociate the dimer into a monomer, which are consistent with our ITC analysis showing K_d values in the micro-molar range [Fig. 3(a) and Table II]. SEC of a full-length DGKα was also performed in the presence of $CaCl_2$ or EGTA [Fig. 4(d)]. Notably, full-length DGK (85 kDa) eluted as a monomer under both conditions, suggesting that although DGKα-EF also undergoes a conformational change in the context of full-length protein, the dimer formation of DGKα-EF is probably an artificial product due to its isolation from a full-length protein.

To test whether DGKα-EF underwent a conformational change upon Ca^{2+} binding, we performed limited proteolysis experiments (Fig. 5). SDS-PAGE after trypsin treatment showed that while calcium binding prevented DGKα-EF from proteolysis, DGKα-EF in the absence of Ca^{2+} was more susceptible to proteolysis, producing peptide species smaller than a full-length protein [Fig. 5(a)]. Subsequent mass spectrometry analysis revealed that those peptide species were produced by trypsin cleavage within helices α1 (at K120), α2 (at R144), and α3 (at R182) [Fig. 5(b,c)]. Circular dichroism spectra of DGKα-EF were also measured with and without $CaCl_2$. In the absence of $CaCl_2$, DGKα-EF exhibited a spectrum characteristic to α-helix containing proteins with helical content being calculated to be 22.1%. As demonstrated by decreased mean residue ellipticity at 222 nm, the α-helical contents further increased upon addition of $CaCl_2$ (to 31.5% with 100 μM $CaCl_2$) (Fig. S3). Taken together, our analysis suggests that DGKα-EF in its apo-state adopts more open conformation accessible to trypsin, which facilitates dimer formation in those isolated EF-hand domains. Upon binding to Ca^{2+}, DGKα-EF likely folds into a more compact conformation with increased α-helical contents, which prefers to be a monomer.

Discussion

Although the biomedical significance of DGK isozymes has been increasingly recognized,[14–18] there has been very limited progress in elucidating the structural basis for DGK function. No structure is available for the catalytic domain of mammalian DGK isozymes. As a part of our long-standing goal of the structural determination of DGKα, we here report the first crystal structure of DGKα-EF in the Ca^{2+}-bound form (Figs. 1 and 2). The structure of Ca^{2+}-bound DGKα-EF displays a pair of helix-loop-helix EF-hand motifs and a canonical Ca^{2+}-coordination. Notably, the existing helix of EF2 is separated to form an additional α5 helix [Figs. 1(c) and 2(a)], which often referred to as a LM helix in other EF-hand domains (Fig. S2 and Table S1). For *Drosophila* Miro which contains two EF-hand motifs sandwiched by two GTPase domains,[43] the LM helix and following linker region are suggested to be responsible for organizing inter-domain arrangement. Thus, it is reasonable to postulate that the hydrophobic LM helix found in the holo-form would play a structurally

Table II. *Thermodynamic Parameters for the Ca^{2+} Binding to DGKα-EF WT and Mutants (E134Q and E179Q)*

		K_d μM (±SD)	ΔH (kcal/mol)	$T\Delta S$ (kcal/mol)	ΔG (kcal/mol)
WT	Site 1	0.32 ± 0.01	−13.40 ± 1.55	−4.53 ± 1.52	−8.87 ± 0.03
	Site 2	2.34 ± 0.91	−5.91 ± 1.07	1.79 ± 0.83	−7.71 ± 0.24
E134Q	(n = 0.96)	31.72 ± 1.66	−3.41 ± 0.45	2.72 ± 0.41	−6.13 ± 0.04
E179Q	(No binding)				

All values shown are average from duplicate runs. n is the binding ratio of Ca^{2+} to DGKα-EF.

important role in the multi-domain organization of DGKα. Interestingly, the amino acids that form the LM helix in DGKα are fully conserved among other Type I DGK isozymes (DGKβ and DGKγ) containing EF-hand domains (Fig. S4).

Unexpectedly, DGKα-EF in its apo-form elutes in a volume corresponding to a dimer [Fig. 4(a,b)]. Limited proteolysis combined with MALDI-TOF MS analysis also shows that DGKα-EF is more susceptible to trypsin digestion in the absence of $CaCl_2$ (Fig. 5). This increased sensitivity to proteolysis in the absence of $CaCl_2$ has been also observed for a DGKα construct containing RVH and EF-hand domains.[34] Some would argue that DGKα-EF is largely unstructured without $CaCl_2$ and has a larger hydrodynamic radius, thus eluting much earlier than that with $CaCl_2$ from SEC. However, unfolding of EF hands in the absence of $CaCl_2$ is a very rare case for EF-hand motifs and our circular dichroism measurement demonstrates that there are no drastic changes in the secondary structure of DGKα-EF in the presence and the absence of $CaCl_2$ (Fig. S3). These results lead us to suggest that the apo-form DGKα-EF adopts a more open conformation with exposed hydrophobic surface, facilitating the dimerization of DGKα-EF. Our previous study using TNS fluorescence has shown that DGKα-EF is more hydrophobic when Ca^{2+} is absent,[33] supporting our proposed explanations. In this regard, we should also note that the dimer formation is highly likely an artificial outcome due to the isolation of EF hands, since a full-length DGKα exists as a monomer under conditions with and without $CaCl_2$ [Fig. 4(d)]. Another notable feature is that, although most of the EF-hand domains adopt a closed conformation when Ca^{2+} ion is absent,[28,36,44] our previous[33] and current studies suggest that DGKα-EF adopts a loosened conformations in the absence of Ca^{2+}, then converted into a compact conformation upon binding to Ca^{2+}. This reflects conformational diversity of EF-hand superfamily proteins.[28] In this context, the α5 LM helix [Fig. 1(b,c)], unique to DGKα-EF and others (Fig. S1 and Table S2), clearly contributes to form a well-packed hydrophobic core of the holo-DGKα-EF and may play a role in the conformational changes from the relaxed apo-form to the holo-form. Structural analysis in the absence of Ca^{2+}, however, is required to clearly define roles of the LM-helix. Unfortunately, our attempt to crystallize the apo-form of DGKα-EF has been unsuccessful to date.

For many instances, EF-hand domains in multi-domain proteins are involved in domain-domain interactions.[45,46] It still remains controversial which domain(s) interacts with DGKα-EF.

In our previous studies, pull-down assays have revealed that, in the absence of $CaCl_2$, GST-fused DGKα-EF interacts with neighboring C1 domains expressed in COS-7 cells and this intramolecular interaction is significantly weakened in the presence of $CaCl_2$.[47,48] On the other hand, Abe et al. have also demonstrated that Ca^{2+}-dependent activation of DGKα is disabled by the mutation of D697 in C-terminal CD, suggesting another model in which N-terminal region including EF-hand domains interacts with CD.[49] We have recently discovered that while a full-length DGKα expressed in insect cells remains a soluble monomer *in vitro*, a protein construct only containing CD (DGKα-CD) forms soluble aggregates upon isolation.[50] This indicates that a potential aggregation-prone surface of DGKα-CD is intra-molecularly buried by the N-terminal regulatory domains including RVH, EF-hands, C1 domain. The crystal structure of DGKα-EF presented here reveals that a large hydrophobic area is clustered nearby N- and C-termini of DGKα-EF when Ca^{2+} ions are bound (Fig. 2), and it is reasonable that the hydrophobic surface mediates intramolecular interactions. Future studies will be required to understand how the conformation of DGKα-EF changes in the absence of Ca^{2+}, and DGKα-EF is involved in domain–domain communications that keeps DGKα in its auto-inhibition state.

In summary, we here report the first crystal structure of DGKα-EF in its Ca^{2+}-bound form. The structure reveals the characteristic "LM" helix that forms a large hydrophobic surface with other residues. We also demonstrate that DGKα-EF adopts a trypsin-susceptible open conformation in the absence of Ca^{2+} and suggest that Ca^{2+} binding induces substantial conformational changes that possibly involve the hydrophobic packing of the LM helix. These conformational changes likely regulate domain–domain interactions responsible for the enzymatic activation of DGKα. Further biophysical and structural biology approaches, however, are needed to characterize intra-molecular interactions and thus to better understand the molecular mechanism underlying Ca^{2+}-dependent activation.

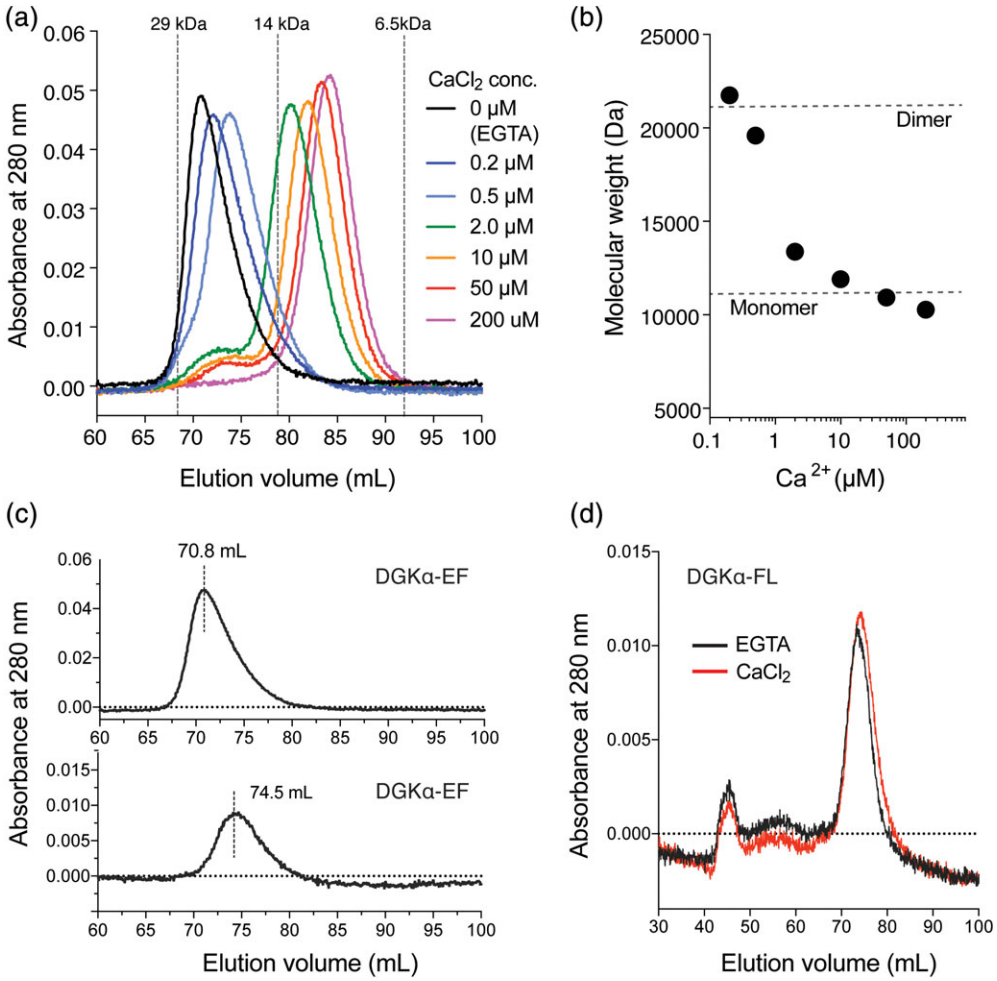

Figure 4. Size-exclusion chromatography (SEC) analysis of DGKα-EF with increasing concentrations of $CaCl_2$. (a) SEC elution profile of DGKα-EF from a Superdex 75 (16/60) column. The column was equilibrated with 20 m*M* Tris–HCl, pH 7.5, 150 m*M* NaCl, 3 m*M* EGTA for the sample without $CaCl_2$. For each SEC experiment with $CaCl_2$, the column was equilibrated with a buffer 1 m*M* EGTA with increasing concentrations of $CaCl_2$. Free Ca^{2+} concentration (0.2–200 μM) was calculated and adjusted from total $CaCl_2$ concentrations in the presence of 1 m*M* EGTA using the Maxchelator program (http://maxchelator.stanford.edu/). DGKα-EF sample (0.4 mg/mL [37.7 μM] × 1.5 mL) was also incubated with respective EGTA/$CaCl_2$ concentrations before chromatography. (b) Effective molecular weight of DGKα-EF as a function of Ca^{2+} estimated the elution volume from the column calibrated with the standard proteins (aldolase (158 kDa), BSA (67 kDa), ovalbumin (44 kDa), carbonic anhydrase (29 kDa), RNase A (13.7 kDa), and aporotinin (6.5 kDa)). (c) Protein concentration dependence of DGKα-EF elution profile in the absence of $CaCl_2$. Concentration and volume of input samples were 0.4 mg/mL (37.7 μM) × 1.5 mL and 0.07 mg/mL (6.6 μM) × 1.5 mL, respectively. (d) Elution profile of a full-length DGKα. Full-length DGKα sample was prepared following our recently published procedure using the baculovirus-insect cell expression system.[50] After Ni^{2+}-affinity chromatography, SEC experiments were performed using a Superdex 200 16/60 column equilibrated with a buffer (20 m*M* Tris–HCl, pH 7.4, 0.2 M NaCl, 3 m*M* $MgCl_2$, 0.5 m*M* DTT, 5% glycerol) containing 3 m*M* $CaCl_2$ or 5 m*M* EGTA. Gel-filtration standards (Bio-Rad) were used to determine the molecular mass of DGKα.

Materials and Methods

Expression and purification of DGKα-EF and its mutants

The gene segment encoding EF-hand domains (E107–E197) of human DGKα (DGKα-EF) flanked by *Nde*I and *Sal*I restriction sites was amplified by PCR using the full-length cDNA for human DGKα as a template. PCR product was inserted into a pSUMO vector, and the pSUMO-DGKα-EF was used to transform *E. coli* strain Rosetta2 (DE3). The protein construct contained a cleavable His-SUMO-tag before the DGKα-EF sequence. Bacterial cells were cultured in Terrific Broth media at 37°C until OD_{600} reached 2.0–2.5. The expression of the recombinant protein was induced by adding 0.2 m*M* isopropyl β-D-thiogalactopyranoside, and the bacterial culture was continued at 37°C for 4 h. Bacteria harvested by centrifugation were suspended in a lysis buffer (50 m*M* sodium phosphate, pH 8.0, containing 300 m*M* NaCl, 10 m*M* imidazole, and protease inhibitor cocktails) and lysed by sonication on ice, and a soluble His_6-SUMO-fused DGKα-EF was purified using Ni-affinity chromatography on Ni-NTA agarose (QIAGEN, Hilden, Germany). Fractions containing His-SUMO-fused DGKα-EF were combined and dialyzed against

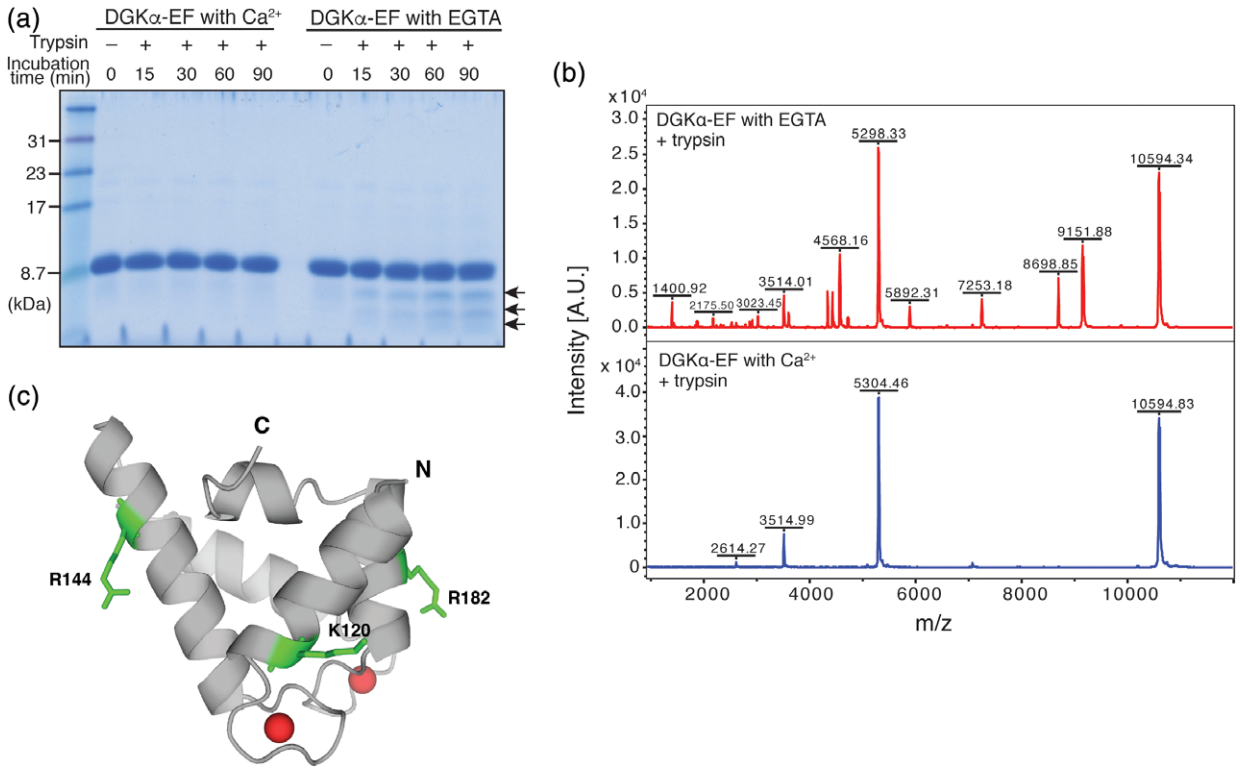

Figure 5. Apo-form DGKα-EF adopts a protease-susceptible conformation. (a) SDS-PAGE analysis of trypsin-limited proteolysis experiment in the presence of $CaCl_2$ or EGTA. The digestion reaction was performed at room temperature and quenched at each time point (15, 30, 60, and 90 min), as shown above the gel, by adding SDS-PAGE loading buffer containing 10 m*M* PMSF. (b) MALDI-TOF MS spectra were acquired on tryptic digests of DGKα-EF in the presence of $CaCl_2$ or EGTA. Peptide fragments with a mass of 9150.4, 8698.4, 7250.5, and 5892.0 were only detected in the sample from the DGKα-EF in its apo-state. (c) Arginine and lysine residues at which trypsin cleavage occurred in the apo-form of DGKα-EF were shown as green sticks and mapped on the holo-form structure. Full-length gel is presented in Fig. S5.

20 m*M* sodium phosphate, pH 8.0, 300 m*M* imidazole. For cleavage of the N-terminal His-SUMO tag, 0.5 μg of ubiquitin-like specific protease (Ulp1) per milligram of the protein was added, and the cleavage reaction mixture was incubated for 2 h at 30°C. The reaction mixture was applied onto a Ni-NTA column, and the flow-through and wash fractions containing the tag-free DGKα-EF was then applied to size-exclusion chromatography on a Superdex 75 column (GE Healthcare, Little Chalfont, UK) equilibrated with 20 m*M* Tris–HCl, pH 7.5, 50 m*M* NaCl. The purity of DGKα-EF was confirmed by SDS-PAGE with Coomassie Brilliant Blue (CBB) staining. Typical yield of the purified protein was ~4 mg of protein per liter of cell culture. Protein concentration was determined by absorbance measurement at 280 nm using an extinction coefficient of 15,470 M^{-1} cm^{-1} or $E_{0.1\%}$ (1 mg/mL) of 1.459 at 280 nm.

DGKα-EF containing E134Q, E179Q, and E134Q/E179Q mutations were prepared by site-directed mutagenesis using KOD-plus polymerase (Toyobo, Osaka, Japan) and *Dpn*I (Takara, Shiga, Japan). The mutations were confirmed by DNA sequencing. Expression and purification of the DGKα-EF mutants were carried out by the same procedure as that used for wild-type protein.

Expression and purification of a full length DGKα

The production of a recombinant full-length DGKα was conducted by following our recently established procedure.[50] Briefly, full length form of DGKα with N-terminal His_6-tag was heterologously expressed in Sf9 insect cells using baculovirus expression vector system and purified using a Ni-NTA column chromatography (QIAGEN). The eluted protein samples were applied to size exclusion chromatography on Superdex 200 16/60 equilibrated with 20 m*M* Tris–HCl, pH 7.4, 200 m*M* NaCl, 3 m*M* $MgCl_2$, 0.5 m*M* dithiothreitol, 5% glycerol with 3 m*M* $CaCl_2$ or 5 m*M* EGTA (GE Healthcare).

Protein crystallization

Crystals of the calcium-bound DGKα-EF were grown using the sitting drop vapor diffusion method at 23°C by mixing the protein solution (9.6 mg/mL) dissolved in 20 m*M* HEPES (Dojindo, Kumamoto, Japan), pH 7.4, 50 m*M* NaCl, 3 m*M* $CaCl_2$ with an equal volume of the reservoir solution containing 0.1 M HEPES, pH 7.0, 1.0 M succinic acid, and 1% (w/v) PEG monomethyl ether 2000 (#34 of Index Crystallization Screens, Hampton Research, Aliso Viejo, CA, USA). Crystals grew within a few days and were

cryo-protected by soaking the crystals in a cryo-protectant solution containing 0.1 M HEPES, pH 7.0, 1.0 M succinic acid (Wako, Osaka, Japan), 2% PEG monomethyl ether 2000 (Hampton Research), and 10% glycerol (Wako). Crystals were then harvested and flash-cooled in liquid nitrogen.

Structure determination and characterization

Native and single-wavelength anomalous diffraction (SAD) data sets were collected from a single crystal at a cryogenic temperature (100 K) on a beam-line BL1A at the Photon Factory (Tsukuba, Japan). The collected data were processed using XDS software[51] and were scaled and merged using XSCALE program.[51] The structure of DGKα-EF was solved by sulfur-SAD phasing method utilizing five intrinsic sulfur atoms in the native protein using AutoSol program.[52] From the experimentally phased maps, the initial structural model was built using AutoBuild program.[53] The structural model was then rebuilt using COOT software,[54] and iteratively refined using PHENIX. refine program.[55] The model was validated using the PROCHECK[56] and RAMPAGE programs.[57] Ramachandran statistics shows that 97.6% of residues are in favored regions, 2.4% in allowed regions, and 0% are outliers. The crystallographic and refinement statistics are summarized in Table I. All structural figures were prepared with the program PyMOL (Schrödinger, LLC, New York, NY, USA). Surface hydrophobicity is visualized based on a normalized consensus hydrophobicity scale[58] using Color_h script in PyMOL (https://pymolwiki.org/index.php/Color_h).

Isothermal titration calorimetry

Calcium binding titrations to DGKα-EF were performed with a MicroCal ITC200 (Malvern Instruments). DGKα-EF was extensively dialyzed against 20 m*M* HEPES buffer, pH 7.4, 50 m*M* NaCl, 5 m*M* EDTA (2 L each time for 12 h and two times) to remove calcium ions bound to the protein during the expression and purification steps, then further dialyzed into 20 m*M* HEPES buffer, pH 7.4, 50 m*M* NaCl (2 L each time for 12 h and four times) to remove EDTA from the sample. $CaCl_2$ was directly dissolved in the buffer used for the dialysis. The protein sample was concentrated to 50 μM using an Amicon Ultra-15 centrifugal filter (EMD Millipore, Burlington, MA, USA). All solutions were filtered through a 0.22 μm membrane filter and degassed for 20 min under vacuum. Titrations of DGKα-EF (300 μL) with 1 m*M* $CaCl_2$ were conducted at 25°C. A total of 20 injections were made. The volume of the first injection was 0.4 μL and that of the following 19 injections were 2 μL. Time interval of 150 sec was used between the injections. Data were fit to an N-identical binding sites model or sequential binding sites model with Origin 7 (OriginLab, Northampton, MA, USA).

Gel filtration chromatography

Gel filtration chromatography was performed on a Superdex 75 16/60 column (GE Healthcare) using a Bio-Logic Duo-Flow FPLC system (BioRad, Hercules, CA, USA) at 4°C to investigate conformational changes and/or oligomerization state of DGKα-EF in response to Ca^{2+} binding.

The column was equilibrated with 20 m*M* Tris–HCl, pH 7.5, 150 m*M* NaCl, 1 m*M* EGTA with increasing concentrations of $CaCl_2$, and ran at a flow rate of 1 mL/min. Free Ca^{2+} concentration (0.2–200 μM) was calculated from total $CaCl_2$ concentrations in the presence of 1 m*M* EGTA using the Maxchelator program (http://maxchelator.stanford.edu/). Gel-filtration standard (BioRad) containing aldolase (158 kDa), BSA (67 kDa), ovalbumin (44 kDa), carbonic anhydrase (29 kDa), RNase A (13.7 kDa), and aporotinin (6.5 kDa) were used as standard proteins to estimate the R_s value of DGKα-EF as a function of Ca^{2+} concentration.

Circular dichroism spectroscopy

Circular dichroism spectra were recorded at ambient conditions between 190 and 250 nm on a Jasco J-805 spectrometer (Jasco Corporation, Tokyo, Japan) using a cell with a path length of 0.2 mm, 20 nm/min scan speed, and a bandwidth of 1 nm. DGKα-EF was prepared at 0.2 mg/mL (18.9 μM) in 20 m*M* Tris–HCl buffer, pH 7.5, with various concentrations of $CaCl_2$ ranging from 0 to 100 μM. Ten spectra were averaged and a spectrum obtained for the buffer was subtracted.

Limited trypsin proteolysis

DGKα-EF was prepared at a protein concentration of 0.6 mg/mL (56.6 μM) in 20 m*M* Tris–HCl, pH 7.5, 150 m*M* NaCl. To the protein solution, $CaCl_2$ or EGTA was added at a final concentration of 5 m*M*. Sequencing grade trypsin (sequencing grade, Promega, Madison, WI, USA) was added to 20 μL of DGKα-EF solution at 1:100 ratio of the trypsin to DGKα-EF. For electrophoresis, reactions were stopped at each time point (15, 30, 60, and 90 min) by adding SDS-PAGE loading buffer containing PMSF (a final PMSF concentration of 10 m*M*) followed by the incubation at 95°C for 10 min, and the reaction products were subjected to Tricine SDS-PAGE analysis with CBB staining. For MALDI-TOF MS (matrix-assisted laser desorption ionization-time of flight mass spectrometry) analysis, 20 μL of reaction mixture was mixed with 8.5 μL of 10% trifluoroacetic acid (TFA) to quench the reaction.

MALDI-TOF MS analysis

MALDI-TOF MS experiments were performed on a Bruker autoflex speed mass spectrometer (Bruker Daltonics, Bremen, Germany) equipped with a Lift mode for MS/MS analysis. The trypsin-treated samples were desalted using C-tip (Nikkyo Technos Co., Ltd., Tokyo, Japan) and eluted with 80% acetonitrile

(Wako, Osaka, Japan) and 0.5% formic acid (Wako, Osaka, Japan). Desalted sample (2 μL) was mixed with 1:1 (v/v) with 2,5-dihydroxybenzoic acid (DHB, Bruker Daltonics, Bremen, Germany), spotted onto a plate (MTP 384 ground steel target plate, Bruker Daltonics) for MALDI-TOF MS, and analyzed using a linear mode. All samples were analyzed under identical instrumental parameters and the instrument was externally calibrated with a set of standard proteins (Protein Mix 1, Bruker). Masses of the trypsin-digested DGKα-EF were calculated and compared with those of observed MS peaks to identify the position of trypsin cleavage.

Acknowledgments

We would like to thank Brandon L Garcia (East Carolina University) for reading the manuscript and useful discussion. The synchrotron radiation experiments were performed at Photon Factory (proposals 2017R-40) and we thank Naohiro Matsugaki and Ayaka Harada for assistance with data collection. This work was supported by Grant-in-Aid for Scientific Research (17K115444 to D.T., 18H05425 to T.M., and 26291017, 15K14470, 17H03650 to F.S.) from Japan Society for the Promotion of Science (JSPS), by Association of Graduate Schools of Science and Technology in Chiba University (D.T.), and the Futaba Electronic Memorial Foundation; the Ono Medical Research Foundation; the Japan Foundation for Applied Enzymology; the Food Science Institute Foundation; the Skylark Food Science Institute; the Asahi Group Foundation and the Japan Milk Academic Alliance (F.S.), and by Platform Project for Supporting Drug Discovery and Life Science Research (Basis for Supporting Innovative Drug Discovery and Life Science Research [BINDS]) from Japan Agency for Medical Research and Development (AMED) under Grant number JP18am0101083 (T.M.).

Protein Data Bank deposition

Atomic coordinates and structure factors for DGKα-EF have been deposited in the RCSB Protein Data Bank with accession code 6IIE.

Conflict of interests

The authors declare no competing interests.

References

1. Sakane F, Imai S-I, Kai M, Yasuda S, Kanoh H (2007) Diacylglycerol kinases: why so many of them? Biochim Biophys Acta 1771:793–806.
2. Mérida I, Ávila-Flores A, Merino E (2008) Diacylglycerol kinases: at the hub of cell signalling. Biochem J 409:1–18.
3. Shulga YV, Topham MK, Epand RM (2011) Regulation and functions of diacylglycerol kinases. Chem Rev 111: 6186–6208.
4. Almena M, Mérida I (2011) Shaping up the membrane: diacylglycerol coordinates spatial orientation of signaling. Trends Biochem Sci 36:593–603.
5. Griner EM, Kazanietz MG (2007) Protein kinase C and other diacylglycerol effectors in cancer. Nat Rev Cancer 7:281–294.
6. Stace CL, Ktistakis NT (2006) Phosphatidic acid- and phosphatidylserine-binding proteins. Biochim Biophys Acta Mol Cell Biol Lipids 1761:913–926.
7. English D (1996) Phosphatidic acid: a lipid messenger involved in intracellular and extracellular signalling. Cell Signal 8:341–347.
8. Parekh DB, Ziegler W, Parker PJ (2000) Multiple pathways control protein kinase C phosphorylation. EMBO J 19:496–503.
9. Newton AC (1997) Regulation of protein kinase C. Curr Opin Cell Biol 9:161–167.
10. Ebinu JO, Bottorff DA, Chan EYW, Stang SL, Dunn RJ, Stone JC (1998) RasGRP, a ras guanyl nucleotide-releasing protein with calcium- and diacylglycerol-binding motifs. Science 280:1082–1086.
11. Tognon CE, Kirk HE, Passmore LA, Whitehead IP, Der CJ, Kay RJ (1998) Regulation of RasGRP via a phorbol ester-responsive C1 domain. Mol Cell Biol 18: 6995–7008.
12. Ávila-Flores A, Santos T, Rincón E, Mérida I (2005) Modulation of the mammalian target of rapamycin pathway by diacylglycerol kinase-produced phosphatidic acid. J Biol Chem 280:10091–10099.
13. Moritz A, De Graan PN, Gispen WH, Wirtz KW (1992) Phosphatidic acid is a specific activator of phosphatidylinositol-4-phosphate kinase. J Biol Chem 267:7207–7210.
14. Noessner E (2017) Diacylglycerol kinase-alpha: a checkpoint in cancer-mediated immuno-inhibition and target for immunotherapy. Front Cell Dev Biol 5:16.
15. Sakane F, Mizuno S, Komenoi S (2016) Diacylglycerol kinases as emerging potential drug targets for a variety of diseases: an update. Front Cell Dev Biol 4:82.
16. Liu K, Kunii N, Sakuma M, Yamaki A, Mizuno S, Sato M, Sakai H, Kado S, Kumagai K, Kojima H, Okabe T, Nagano T, Shirai Y, Sakane F (2016) A novel diacylglycerol kinase α-selective inhibitor, CU-3, induces cancer cell apoptosis and enhances immune response. J Lipid Res 57: 368–379.
17. Purow B (2015) Molecular pathways: targeting diacylglycerol kinase alpha in cancer. Clin Cancer Res 21: 5008–5012.
18. Dominguez CL, Floyd DH, Xiao A, Mullins GR, Kefas BA, Xin W, Yacur MN, Abounader R, Lee JK, Wilson GM, Harris TE, Purow BW (2013) Diacylglycerol kinase α is a critical signaling node and novel therapeutic target in glioblastoma and other cancers. Cancer Discov 3:782–797.
19. Yanagisawa K, Yasuda S, Kai M, Imai S-I, Yamada K, Yamashita T, Jimbow K, Kanoh H, Sakane F (2007) Diacylglycerol kinase α suppresses tumor necrosis factor-α-induced apoptosis of human melanoma cells through NF-κB activation. Biochim Biophys Acta Mol Cell Biol Lipids 1771:462–474.
20. Bacchiocchi R, Baldanzi G, Carbonari D, Capomagi C, Colombo E, van Blitterswijk WJ, Graziani A, Fazioli F (2005) Activation of alpha-diacylglycerol kinase is critical for the mitogenic properties of anaplastic lymphoma kinase. Blood 106:2175–2182.
21. Takeishi K, Taketomi A, Shirabe K, Toshima T, Motomura T, Ikegami T, Yoshizumi T, Sakane F, Maehara Y (2012) Diacylglycerol kinase alpha enhances hepatocellular carcinoma progression by activation of Ras-Raf-MEK-ERK pathway. J Hepatol 57:77–83.

22. Torres-Ayuso P, Daza-Martín M, Martín-Pérez J, Ávila-Flores A, Mérida I (2014) Diacylglycerol kinase α promotes 3D cancer cell growth and limits drug sensitivity through functional interaction with Src. Oncotarget 5: 9710–9726.
23. Mérida I, Torres-Ayuso P, Ávila-Flores A, Arranz-Nicolás J, Andrada E, Tello-Lafoz M, Liébana R, Arcos R (2017) Diacylglycerol kinases in cancer. Adv Biol Regul 63:22–31.
24. Jones DR, Sanjuan MA, Stone JC, Mérida I (2002) Expression of a catalytically inactive form of diacylglycerol kinase a induces sustained signaling through RasGRP. FASEB J 16:595–597.
25. Zha Y, Marks R, Ho AW, Peterson AC, Janardhan S, Brown I, Praveen K, Stang S, Stone JC, Gajewski TF (2006) T cell anergy is reversed by active Ras and is regulated by diacylglycerol kinase-alpha. Nat Immunol 7: 1166–1173.
26. Olenchock BA, Guo R, Carpenter JH, Jordan M, Topham MK, Koretzky GA, Zhong X-P (2006) Disruption of diacylglycerol metabolism impairs the induction of T cell anergy. Nat Immunol 7:1174–1181.
27. Sakane F, Yamada K, Kanoh H, Yokoyama C, Tanabe T (1990) Porcine diacylglycerol kinase sequence has zinc finger and E-F hand motifs. Nature 344:345–348.
28. Yap KL, Ames JB, Swindells MB, Ikura M (1999) Diversity of conformational states and changes within the EF-hand protein superfamily. Proteins 37:499–507.
29. Johnson CN, Damo SM, Chazin WJ (2014) *EF-hand calcium-binding proteins*. In: eLS John Wiley & Sons Ltd: Chichester DOI: https://doi.org/10.1002/9780470015902.a0002712
30. Kawasaki H, Kretsinger RH (2017) Structural and functional diversity of EF-hand proteins: evolutionary perspectives. Protein Sci 26:1898–1920.
31. Sakane F, Yamada K, Imai S-I, Kanoh H (1991) Porcine 80-kDa diacylglycerol kinase is a calcium-binding and calcium/phospholipid-dependent enzyme and undergoes calcium-dependent translocation. J Biol Chem 266: 7096–7100.
32. Sakane F, Imai S-I, Yamada K, Kanoh H (1991) The regulatory role of EF-hand motifs of pig-80k diacylglycerol kinase as assessed using truncation and deletion mutants. Biochem Biophysi Res Commun 181:1015–1021.
33. Yamada K, Sakane F, Matsushima N, Kanoh H (1997) EF-hand motifs of α, β and γ isoforms of diacylglycerol kinase bind calcium with different affinities and conformational changes. Biochem J 321:59–64.
34. Jiang Y, Qian W, Hawes JW, Walsh JP (2000) A domain with homology to neuronal calcium sensors is required for calcium-dependent activation of diacylglycerol kinase α. J Biol Chem 275:34092–34099.
35. Merino E, Sanjuán MA, Moraga I, Ciprés A, Mérida I (2007) Role of the diacylglycerol kinase alpha-conserved domains in membrane targeting in intact T cells. J Biol Chem 282:35396–35404.
36. Gifford JL, Walsh MP, Vogel HJ (2007) Structures and metal-ion-binding properties of the Ca^{2+}-binding helix–loop–helix EF-hand motifs. Biochem J 405:199–221.
37. Yap KL, Ames JB, Swindells MB, Ikura M (2002) Vector geometry mapping. A method to characterize the conformation of helix-loop-helix calcium-binding proteins. Methods Mol Biol 173:317–324.
38. Holm L, Rosenström P (2010) Dali server: conservation mapping in 3D. Nucleic Acids Res 38:W545–W549.
39. Shojima T, Hou F, Takahashi Y, Matsumura Y, Okai M, Nakamura A, Mizuno K, Inaba K, Kojima M, Miyakawa T, Tanokura M (2018) Crystal structure of a Ca^{2+}-dependent regulator of flagellar motility reveals the open-closed structural transition. Sci Rep 8(1): 2014–2012.
40. Ishida H, Jensen KV, Woodman AG, Hyndman ME, Vogel HJ (2017) The calcium-dependent switch helix of L-plastin regulates actin bundling. Sci Rep 7: 213492–213412.
41. Park KR, Kwon M-S, An JY, Lee J-G, Youn H-S, Lee Y, Kang JY, Kim TG, Lim JJ, Park JS, Lee SH, Song WK, Cheong HK, Jun CD, Eom SH (2016) Structural implications of Ca^{2+}-dependent actin-bundling function of human EFhd2/Swiprosin-1. Sci Rep 6:1–15.
42. Aurelius O, Johansson R, Bågenholm V, Lundin D, Tholander F, Balhuizen A, Beck T, Sahlin M, Sjöberg B-M, Mulliez E, Logan DT (2015) The crystal structure of *Thermotoga maritima* class III ribonucleotide reductase lacks a radical cysteine pre-positioned in the active site. PLoS One 10:e0128199–e0128120.
43. Klosowiak JL, Focia PJ, Chakravarthy S, Landahl EC, Freymann DM, Rice SE (2013) Structural coupling of the EF hand and c-terminal GTPase domains in the mitochondrial protein Miro. EMBO Rep 14:968–974.
44. Lewit-Bentley A, Réty S (2000) EF-hand calcium-binding proteins. Curr Opin Struct Biol 10:637–643.
45. Iwasaki W, Sasaki H, Nakamura A, Kohama K, Tanokura M (2003) Metal-free and Ca^{2+}-bound structures of a multidomain EF-hand protein, CBP40, from the lower eukaryote *Physarum polycephalum*. Structure 11:75–85.
46. Klosowiak JL, Park S, Smith KP, French ME, Focia PJ, Freymann DM, Rice SE (2016) Structural insights into parkin substrate lysine targeting from minimal Miro substrates. Sci Rep 6:257–213.
47. Takahashi M, Yamamoto T, Sakai H, Sakane F (2012) Calcium negatively regulates an intramolecular interaction between the N-terminal recoverin homology and EF-hand motif domains and the C-terminal C1 and catalytic domains of diacylglycerol kinase α. Biochem Biophys Res Commun 423:571–576.
48. Yamamoto T, Sakai H, Sakane F (2014) EF-hand motifs of diacylglycerol kinase interact intramolecularly with its C1 domains. FEBS Open Bio 4:387–392.
49. Abe T, Lu X, Jiang Y, Boccone CE, Qian S, Vattem KM, Wek RC, Walsh JP (2003) Site-directed mutagenesis of the active site of diacylglycerol kinase alpha: calcium and phosphatidylserine stimulate enzyme activity via distinct mechanisms. Biochem J 375:673–680.
50. Takahashi D, Sakane F (2018) Expression and purification of human diacylglycerol kinase α from baculovirus-infected insect cells for structural studies. PeerJ 6: e5449–e5418.
51. Kabsch W (2010) XDS. Acta Crystallogr D66:125–132.
52. Terwilliger TC, Adams PD, Read RJ, McCoy AJ, Moriarty NW, Grosse-Kunstleve RW, Afonine PV, Zwart PH, Hung LW (2009) Decision-making in structure solution using Bayesian estimates of map quality: the PHENIX AutoSol wizard. Acta Cryst D65:582–601.
53. Terwilliger TC, Grosse-Kunstleve RW, Afonine PV, Moriarty NW, Zwart PH, Hung LW, Read RJ, Adams PD, IUCr (2008) Iterative model building, structure refinement and density modification with the PHENIX AutoBuild wizard. Acta Crystallogr D64:61–69.
54. Emsley P, Cowtan K (2004) Coot: model-building tools for molecular graphics. Acta Crystallogr D60:2126–2132.
55. Adams PD, Afonine PV, Bunkoczi G, Chen VB, Davis IW, Echols N, Headd JJ, Hung LW, Kapral GJ, Grosse-Kunstleve RW, McCoy AJ, Moriarty NW, Oeffner R, Read RJ, Richardson DC, Richardson JS, Terwilliger TC, Zwart PH (2010) PHENIX: a comprehensive Python-based system for macromolecular structure solution. Acta Cryst D66:213–221.

56. Laskowski RA, MacArthur MW, Thornton JM (1998) Validation of protein models derived from experiment. Curr Opin Struct Biol 8:631–639.
57. Lovell SC, Davis IW, Arendall WBIII, de Bakker PIW, Word JM, Prisant MG, Richardson JS, Richardson DC (2003) Structure validation by C alpha geometry: phi, psi and C beta deviation proteins. 50:437–450.
58. Eisenberg D, Schwarz E, Komaromy M, Wall R (1984) Analysis of membrane and surface protein sequences with the hydrophobic moment plot. J Mol Biol 179:125–142.